HOT WIRE ANEMOMETRY

by

Peter Walter Becker

Submitted in Partial Fulfillment of the Requirements

for the degree of

Master of Science in Engineering

in the

Mechanical Engineering

Program

Dennis Torok — 21, May 73

Adviser — Date

Edwin R Pejack — 21 May 73

Adviser — Date

Karl E Kiel — June 1, 1973

Dean — Date

YOUNGSTOWN STATE UNIVERSITY

June, 1973

ABSTRACT

HOT WIRE ANEMOMETRY

Peter Walter Becker

Master of Science in Engineering

Youngstown State University, 1973

An extremely accurate method for measuring flow velocities in liquids and gases is by the use of a hot wire anemometer. In this study a technique is developed to calibrate a hot film anemometer in water at intermediate velocities. The voltage output of the anemometer is monitored by either a digital display or Brush Recorder.

The velocity field is created by drawing the probe through a water tank and simultaneously drawing along with it a contact point sliding over a coil of wire generating a frequency proportional to the probe velocity. The velocity range of the system extends from a lower value of 30 cm./sec. to an upper limit of approximately 95 cm./sec.

Calibration curves are generated for various overheat ratios along with a curve relating probe resistance with probe temperature. A curve is also developed for the case when the probe is at a 45° angle with respect to the velocity flow.

ACKNOWLEDGEMENTS

The author wishes to thank his advisers, Dr. Dennis Torok and Dr. E. Pejack for their help in this investigation. Thanks also go to Rick McKee, Jerry Pizzo, Kathy Keaveny and Nancy Woebkenberg, for their help in preparing the manuscript.

TABLE OF CONTENTS

TABLE OF CONTENTS

LIST OF SYMBOLS

SYMBOL	DEFINITION	UNITS OR REFERENCE
Cp	Specific heat	Joule/gm-deg
E	Mean voltage	Volt
Eb	Mean bridge voltage	Volt
Er	Mean reference voltage	Volt
Es	Sensor voltage	Volt
Gr	Grashof number	-
g	Gravity acceleration	cm/sec^2
h	Convective heat transfer coefficient	$Watt/cm^2deg$
Nu	Nusselt No.	-
Pr	Prandtl No.	-
Ro	Sensor Resistance	ohm
Rs	Sensor Resistance	ohm
Rsr	Reference sensor resistance	ohm
R_3	Bridge leg resistance	ohm
R	Sensor Resistance	ohm
T	Fluid Temperature	^oC
Ta	Ambient fluid temperature	^oC
T_o	Reference temperature	^oC
Ts	Sensor temperature	^oC
TsR	Reference sensor temperature	^oC
U	Velocity	cm/sec

LIST OF SYMBOLS

SYMBOL	DEFINITION	UNITS OR REFERENCE
β	Expansivity of fluid	$1/^{o}c$
β_o	Sensor coefficient of resistance	$1/^{o}c$
η	Temperature level $\frac{Ts + T\infty}{2}$	^{o}C
K	Thermal diffusivity	-

LIST OF FIGURES

CHAPTER I

Introduction

The objective of this work is to develop an accurate hot film calibration which can be used to measure velocity in a liquid. Various schemes are in use today depending on the fluid to be measured and the facilities available.

One frequently used method is to locate the sensing probe in the stream of a water jet. The jet stream is located at the bottom of a holding tank. The velocity control is the height to which the level is allowed to stand above the center-line of the jet stream where the probe is located. From Bernoullis theorem we get

$$u = \sqrt{2gh} \qquad (1)$$

where u is the average jet velocity and h is the free height above the jet. This type of apparatus requires a holding tank and a return pump system. A filter should also be placed in the line along with a valve to regulate the height h. A well designed orifice should be placed in the jet to insure that the probe is sensing in a streamline flow. The chief limitation of this apparatus is that it becomes very inaccurate for

velocities below 90 cm./sec. because at this range the surface height h becomes of the order of magnitude of the orifice diameter. This can be deduced from equation 1. Surface effects such as ripple and slosh can affect readings at this height and can result in uneven jet flow.

Another method of calibration is the rotating water tank. A cylindrical tank of water with a vertical axis is made to rotate at a speed about its axis. Due to the skin friction the water at the outer edges of the surface will spin at the tangential velocity of the cylinder. After sufficient time the entire cylinder of water will act as a solid disk rotating at the angular velocity of the cylinder. For this arrangement the velocity varies linearly outward from 0 at the center, to WR at the walls of the tank, where R is the radius of the tank and W is the angular velocity of the tank. For solid body rotation the velocity of the liquid is then known.

Usually for this method small volumes of water are used and therefore the water must be changed often to keep down the effects of contaminants. This small volume of water however has two advantages. It can be drained easily and if the fluid is expensive it requires less liquid to be purchased. Another advantage is the accuracy with which the velocity can be known.

Another method used is simply moving a container of liquid past the stationary probe. This method derives its driving force to lift the liquid from a counterweight which can be varied to give a range of velocities from 0 to a value depending on the height of the liquid container. Limitations are created by the mass of water to be moved and the distance available in which to accelerate the water to the desired velocity. This method is well suited for low velocity investigations. The counterweight can be so chosen that extremely low velocities are reached with very smooth operation.

The last method considered is the towing tank. This consists basically of a tank of some length, opened at the top with a rail system which supports a probe and allows the prove to be drawn through the water at a known velocity. This method was used to calibrate the hot wire anemometer in this work and will therefore be covered more fully in the body of this work.

A table of comparisons may be helpful at this point and is given below.

TABLE 1

COMPARISON OF CALIBRATION METHODS

Method	Vel. Range	Comments
Jet Stream	90-350 cm./sec.	Accurate at high velocities
Rotating Tank	0-WR $R \simeq 50$CM. $W < 1800$RPM	Small liquid volume
Vertical Lift	0-90 cm/sec.	Impractical at high velocities
Towing Tank	30-95 cm./sec.	Large volume of liquid required

CHAPTER II

GENERAL THEORY

General Principles

There are two types of anemometers available. One is the constant temperature anemometer (CTA) and the other is the constant current anemometer (CCA). The CCA maintains the current in the probe at a constant level while the flow field changes the resistance of the probe along with its temperature.

In the CTA system current passing through a probe heats the probe to a certain temperature above the liquid's temperature. The ratio of probe temperature to fluid temperature is called the overheat ratio. Heat is transferred to the passing fluid and the amount transferred is proportional to the temperature difference which is proportional to the stream velocity. The amount of voltage required to maintain a constant probe temperature is calibrated as the free stream velocity.

There are four major areas of concern as found in previous studies with hot wire anemometers. One problem is drift. Drift can be caused by several sources. Electronic instability such as diode heating can affect consecutive readings. This source of drift can often be relieved by

simply allowing the instrument to come to thermal equilibrium after an hour or so. Another source of drift can be electrochemical corrosion on the probe structure. By far the most significant cause of drift is surface fouling. This can be eliminated by proper probe design and maintenance care on the probe. Surface fouling changes the heat transfer characteristics of the probe. Since contaminants in the liquid vary in size and material corrections for these insulating effects are difficult to predict and no one calibration is sufficient for accurate use.

Another area of concern is sensitivity. The sensitivity of a CTA probe is usually given as the rate of change of voltage output with velocity holding temperature constant. The sensitivity of a CCA system is defined as the rate of change of voltage output with a change in temperature holding velocity constant. As will be seen in this investigation the sensitivity changes with the various overheat ratios used.

In the calibration process for a constant temperature anemometer it is convenient to plot the calibration surface as a probe voltage output versus fluid velocity with the stream temperature as constant during calibration. This method is useful in mean stream velocity calibration.

In the calibration process for velocity fluctuations a direct approach is even more difficult. In liquid streams

such as water the frequency fluctuations are less than that in air and can be simulated by a square wave test in which a signal is introduced into the bridge circuit to approach realistic velocity variations. This has its shortcomings in that time delay effects from probe interference are not accounted for.

Another area of concern which exists in many sensing situations is the noise from non-related source. Noise can be the result of either mechanical or electrical generation sources. Electrically, radiation or ground loops can create noise. Impure water as a conductor allows a ground loop to be formed through the water. This ground loop can connect an external power source with the probe. Mechanically noise is created by vibrational problems. Many types of filters are available to cut down the effect of noise.

Basic Anemometer Theory

The basic driving force in the response of a constant temperature anemometer is the heat transfer between the sensor and the passing fluid. This heat transfer is dependent upon the fluid stream velocity, the temperature difference between the sensor and stream and the physical properties of the sensor.

Ostrach and McAdams have shown that the Reynolds number, Nusselt number, Prandtl and Grashof numbers are significant in describing heat flow from the sensor

Along with the above parameters the assumption is made that the flow over the probe is laminar regardless of turbulence anywhere else in the fluid.

The Nusselt number can be expressed as dependent on bridge voltage E_b.

$$q = \frac{E_S^2}{R_S} = hA(T_S - T_\infty) \tag{2}$$

here q is the sensor heat loss and A is the heating surface area. From equation isolation done by Goodman[1], the Nusselt number is given by

$$Nu = .42 Pr^{.2} + .57 Pr^{.33} RE^{.5} \tag{3}$$

only when

$$RE > .5 \quad AND \quad GR \times PR < 10^4 \tag{4}$$

Professor L. V. King derived and experimentally verified an expression relating heat transferred from a heated sensor to air velocity. King's law is given as

---

[1] C.H. Goodman, "Calibration of a Hot Film Anemometer in Water Over the Velocity Range", (Ph.D. Thesis, Mech. Engr. Dept., Tulane Univ., 1970), P. 90.

$$I^2R = (R - R_E)(A + B\sqrt{Re}) \qquad (5)$$

where A,B are constants which vary with sensing wires and fluid properties, Re is the Reynolds number, I is the hot wire current, R is hot wire resistance and R_E is the unheated wire resistance. Experimentation proved this law valid for a variety of Reynold's numbers and a velocity range from 0 -- 6100 cm./sec. For incompressible, steady temperature, steady composition flow, eq. 5 becomes

$$C = C_o\left[\left(\frac{I}{I_o'}\right) - 1\right]^2 \qquad (6)$$

where C is the cooling velocity, Co is a calibration constant, I is the wire current, Io is the current at zero velocity.

Anemometer Circuitry

Two types of measuring circuits are available in anemometry. One is a constant current anemometer circuit while the other is a constant temperature anemometer circuit. In this work the constant temperature circuit is the type used and is shown in Fig. 1. At the balanced bridge state the D. C. amplifier provides a bridge across arms AC. As the fluid passes by the sensor it tends to cool the sensor and

unbalance the bridge. A feedback system amplifies this unbalance and the sensor temperature is brought back up to its initial constant value. The output of the anemometer system is therefore the output of the voltage amplifier which is actually the voltage E_B which provides the necessary current to heat the sensor. The bridge voltage E_B is related to sensor voltage E_S by the bridge formula. (See Fig. 1).

$$E_b = \frac{(R_s + R_3)\, E_s}{R_s} \tag{7}$$

Where E_B, E_S, R_S, and R_3 are shown on the circuit schematic. As mentioned previously the sensor temperature is set at some temperature higher than the fluid temperature. This is done by adjusting resistance R_2. In most cases the relationship between R_S and sensor temperature T_S is.

$$R_s/R_o = 1 + \beta_o (T_s - T_o) \tag{8}$$

The subscript 0 refers to the reference temperature while Ro is the sensor resistance, and β_o is the temperature coefficient of resistance at the reference temperature T_o.

Probes

Many types of probes are currently available for use. The simplest are hot wire probes where fine wire is supported

by a suitable modified set of prongs. These hot wire probes are used mainly in air and are generally not rugged enough for liquid use. For fluids such as water a quartz coated probe is generally used. A fine metal film is covered with quartz which insulates it and also helps maintain some corrosive resistance. In this investigation a hot film probe was used.

Fig. 3 shows how the hot film probe was mounted onto the sliding pad. This figure shows the coil contact arrangement.

Temperature Effects

In the transition from laboratory conditions to actual flow measurements where temperatures cannot be controlled, a mathematical tool will be required to facilitate the use of laboratory calibrations.

Following the work of Goodman let us establish two variables in addition to the fluid velocity, sensor temperature and free stream temperature. Let us define

$$\xi = T_s - T_\infty \tag{9}$$

$$\eta = \frac{T_s + T_\infty}{2} \tag{10}$$

Again to facilitate the generation of a calibration curve a standard bridge voltage will be introduced which relates the

laboratory calibration to a fixed reference set (Rs_R, T_R). Based on these definitions Goodman arrives at

$$E_R = E_B \left(\frac{Rs_R + R3}{Rs + R3} \right) \left(\frac{\xi_R Rs}{\xi Rs_R} \right) \qquad (11)$$

This result is therefore useful in applying the laboratory calibration to field application. E_R is equal to E_B in this investigation because Rs_R, the reference temperature resistance is equal to Rs, the sensor resitance. In general Rs_R does not equal Rs, and ξ_R does not equal ξ because field applications do not generally occur with fluids whose temperatures are equal to the reference temperature of the laboratory.

CHAPTER III

WATER CIRCUIT

General Description

As was mentioned in the introduction, the method of calibration used was the towing tank. The tank itself is a one ft. by one ft. by four ft. long tank made of clear plexiglas. The tank is mounted on a wooden board for stability. On the top of this tank is mounted a track with adjacent coil used as a frequency generator. On this track is fitted a pad which supports the probe. The pad is drawn by a cord attached to a pulley which draws the pad a various linear velocities from approximately 30 cm./sec. to 90 cm./sec. See Fig. 4 for a schematic of the drawing tank system.

Coil Calibration

In order to insure that the tank was long enough to allow the probe to reach a constant velocity for some distance, dry runs with the probe were made. The input voltage to the D. C. drive motor was varied from 10 volts to 60 volts. The results of these runs are shown in Appendix A, Fig. 5.

These data points were found by the following method. The coiled frequency generator has 5 coils/in. and the

resulting frequency is displayed on a Brush Recorder. The strip chart output is then analyzed by noting the chart speed used which was 125 mm./sec. By dividing the total chart into some convenient time intervals a frequency can be counted per given time. This frequency is then converted into cm./sec. In Fig. 6 a typical strip chart output is shown with time scale marked off.

Let us use Fig. 6 as an example of the above method. For a chart speed of 125 mm./sec. and one major division being 5 mm., this major division then represents

$$\frac{5\,\text{MM}}{125\,\text{MM/SEC.}} = .04\,\text{SEC.} \qquad (12)$$

Counting the number of contacts made during this time interval from the coil velocity output between the lines as indicated in Fig. 6 one gets three cycles. Recalling that each cycle represents 0.2 inch.

$$\frac{3\,\text{CYCLES} \times .2\,\text{IN/CYCLE} \times 2.54\,\text{CM./IN.}}{.04\,\text{SEC.}} = \frac{38.1\,\text{CM}}{\text{SEC}} \qquad (13)$$

This final calculation gives the velocity of the probe as indicated by the coil velocity output in Fig. 6.

Start-up Procedure

Initial tests were run to determine the effect of probe water resistance on the velocity output. Strip chart outputs were compared with and without the probe. No difference was noted. Any deviation would automatically be accounted for because the coil's output is an independent velocity for each run. This velocity was used to draw the calibration charts and would eliminate any error due to drag differences.

After the above background is insured preparations for data runs began with a warm-up of all electrical machinery and instruments. For detailed instructions on the operating procedure see DISA Manual. Next, the probe was secured to the sliding block and placed far enough below the surface of the water so that surface effects did not influence the probe's output. This depth was approximately 3 inches.

In order to insure accurate coil frequency counts, the dowel with the wire wrappings was sprayed with seven coats of lacquer varnish and sand-papered along the contact line only. This insured a constant coil spacing of .2 in. and also made the contact operation a smoother one.

For a listing of apparatus used in the data runs see Appendix B, page 36.

After initial preparations are made, data runs were begun with three overheat ratios and various probe positions. These results are given in Appendix A.

System Limitations

The principal limitations in the above system are in the limits of velocities available. Below 30 cm./sec. the probe begins to sense the vibrations from the frequency contact point and it becomes difficult to monitor the output voltage of the probe on a chart recorder. At the upper velocity range of 90 cm./sec., it becomes difficult to count the number of contacts made by the contact point. For high velocities the length of the tank begins to make the attainment of steady state conditions difficult. These considerations therefore limit the velocity range from 30 cm./sec. to 90 cm./sec.

CHAPTER IV

CALIBRATION

Velocity Calibration

The actual calibration process was carrried out by using the water temperature of 18.3°C (67°F) as the reference temperature. Initially in order to establish the relationship between a laboratory calibration and an application where the probe is used at a temperature other than at the reference temperature, a curve of sensor temperature versus sensor resistance is required. This curve is given in Fig. 2 From the curve and from eq. 8 we get

$$R_s/R_o = 1 + \beta_o(T_s) \qquad T_o = 0 \tag{14}$$

$$R_s = R_o(1 + \beta_o T_s) \tag{15}$$

Ro is the extrapolated resistance of the probe at zero degrees centigrade.

$$R_s = R_o + R_o \beta_o T_s \tag{16}$$

$$\beta_o = .00341 = 1/294 \tag{17}$$

As given in Fig. 2 the sensor resistance can now be calculated.

The probe output as seen in Fig. 6 begins at an initial output voltage. In the previous example it was 4.4 volts. The minor divisions are given as .5 volt/division. In the probe output trace, the recorder was displayed approximately 8.5 divisions or

$$8.5\ \text{DIV.} \times \frac{.5\ \text{VOLT}}{\text{DIV.}} = 4.25\ \text{VOLT} \qquad (18)$$

adding this to the base line voltage of 4.4 volts one gets 8.65 volts.

Discussion of Calibration Curves

Fig. 7 shows a calibration curve for a DISA type 55A87 nickel film and quartz coated probe. An initial overheat ratio of 1.1 was selected resulting in the illustrated curve with a sensitivity of .0183 volts/cm./sec. Fig. 8 shows a group of three curves with indicated overheat ratios. As expected the sensitivity increases with overheat ratio but is limited by surface boiling effects which occur when the probe temperature is too high with respect to the flow pattern. Fig. 9 is a comparison between calibrations at an overheat ratio of 1.1 with the probe mounted axially and at a 45° angle with the flow. The increase in sensitivity may be due to turbulence created over the quartz coating resulting in

partial cavitation at higher velocity.

Since the cone shaped body now lies at a 45° angle with the flow, the stream no longer sees a favorable path for laminar flow around the probe. This situation can be similar to an airfoil. At one face of the cone, similar to the bottom of an airfoil, laminar flow is generally maintained. On the opposite face of the cone which can be compared to the top of the airfoil, laminar flow is difficult to maintain at a 45° angle. This results in flow separation and also a change in the fluid's film coefficient. Since the film coefficient increases slightly, the sensitivity also increases. This is seen in Fig. 9, page 33, where the curve for the probe at 45° has a sharper slope.

Fig. 10 is a curve showing how the probe sensitivity varies with the overheat ratio. As explained before, the upper limit on the practical overheat ratio results from effects of surface boiling.

CHAPTER V

RESULTS AND CONCLUSION

The results of the calibration technique are given in Table 2 P. 21 and in the curves in Appendix A. From tests run on the system the velocity range available was from 38.1 cm./sec. to 89.1 cm./sec.

From the data for sensor resistance and sensor temperature, the equation relating the two terms was found to be

$$R_S = 19.65 + .067 T_S \tag{19}$$

$$T_S = 15 R_S - 294 \tag{20}$$

The greatest sensitivity $\left.\frac{\partial E_B}{\partial u}\right|_{T=C}$ was found at an overheat ratio of 1.125 to be .0214 volts/cm./sec. The actual calibration curves can be found in Appendix A.

From Fig. 10 it was observed that an increase in the overheat ratio resulted in an increase in sensitivity. As was mentioned in the theory, the driving force in the response of a CTA system is the heat transferred to the fluid. A higher overheat ratio creates a greater temperature difference and thereby increases the heat transferred for equivalent velocities. This fact increases the sensitivity

TABLE 2

CALIBRATION DATA

$T_S = Ts_R$ $R_S = Rs_R$ $E_R = E$

RUN	RUN #1	RUN #2	RUN #3	RUN #4
Overheat Ratio	1.100	1.125	1.050	1.100
Water Temp.	18.3°C	18.3°C	18.3°C	18.3°C
T_s	20.1°C	20.6°C	19.2°C	20.1°C

	RUN #1		RUN #2		RUN #3		RUN #4	
MOTOR VOLTAGE	VELOCITY cm./sec.	E_B volts	VELOCITY cm./sec.	E_B volts	VELOCITY cm./sec.	E_B volts	VELOCITY cm./sec.	E_B volts
15	38.1	7.95	44.6	9.14	38.1	5.74	38.1	7.39
20	50.6	8.30	51.0	9.39	50.8	5.90	50.5	7.64
30	61.2	8.41	63.5	9.77	63.4	6.10	61.2	7.89
40	76.2	8.71	76.4	9.94	76.2	6.30	76.2	8.38
50	89.0	8.90	82.8	10.29	89.0	6.50	89.1	8.54

to some point where surface boiling begins to become a problem. As the heat transfer to the fluid is increased more current is required to maintain the bridge balance and thus the value of Eb is higher for an increased overheat ratio in an equivalent flow field.

The upper velocity range for the equipment used was mechanically limited by the electric motor used to drive the pulley which towed the probe. Applied voltage over 50 volts made little increase in towing velocity. Monitoring limitations arose from the Brush Recorder used whose maximum chart speed was only 125 mm./sec. A higher chart speed would make coil velocity data much more readable and accurate. The Brush Recorder also limited the accuracy with which the probe's output was recorded. More sensitivity would have been required from the channel carrying the probe signal. As with the Brush Recorder available being the weakest device in terms of accuracy, the error introduced could have been a half division over a scale of 10 divisions which alone would account for a 5% error in strip chart reading.

In Fig. 11 one can see how the Brush Recorder output becomes more difficult to read. At 40 volts there are approximately 5 contacts per .04 seconds. At 15 volts there are 3. Higher velocities would become very difficult to

read and would have less accuracy with this Brush Recorder. A higher chart speed would increase the accuracy. An estimated error of ½ cycle out of 6 contacts would add another 8% error to the results.

APPENDIX A

System and Figures

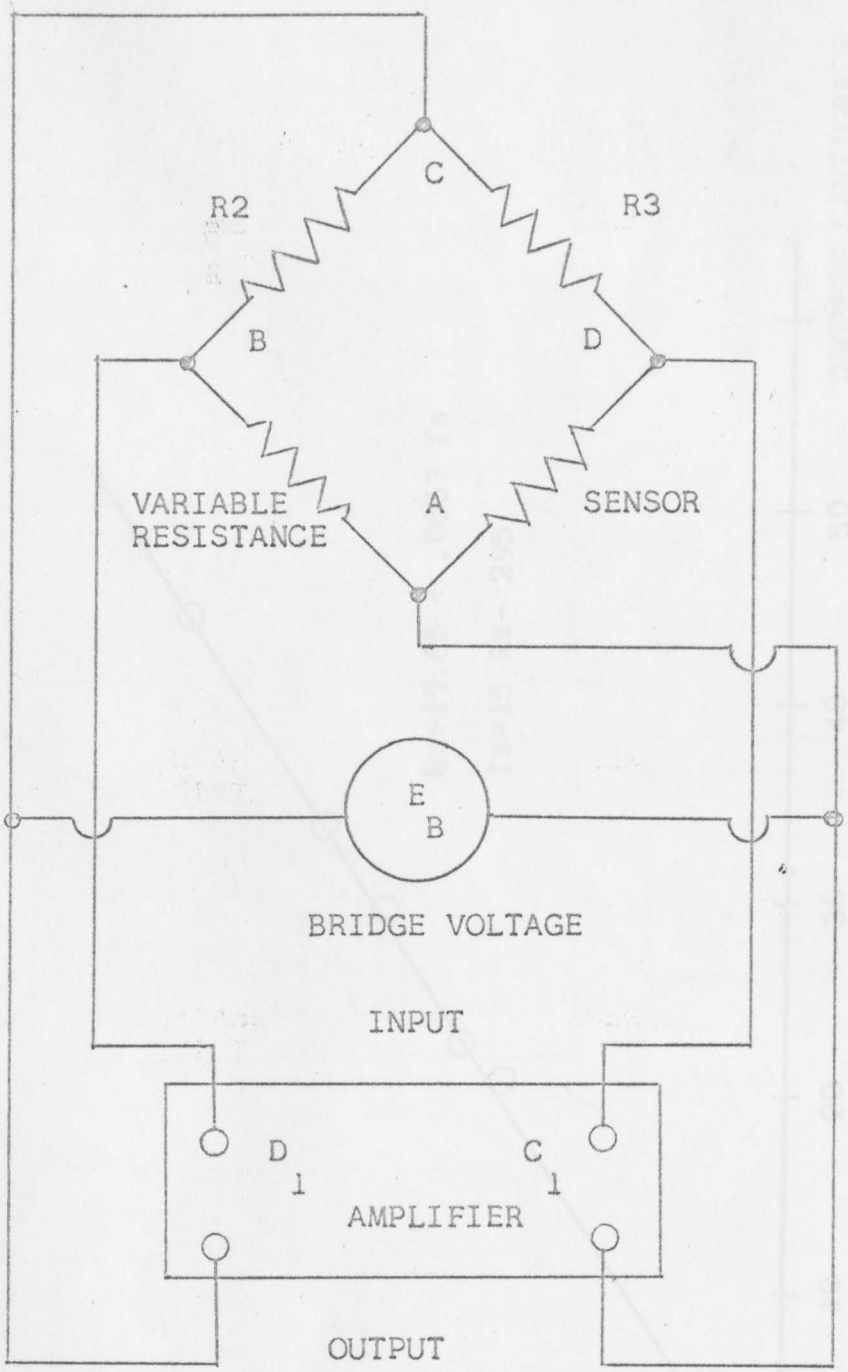

Fig.1. Electrical Schematic

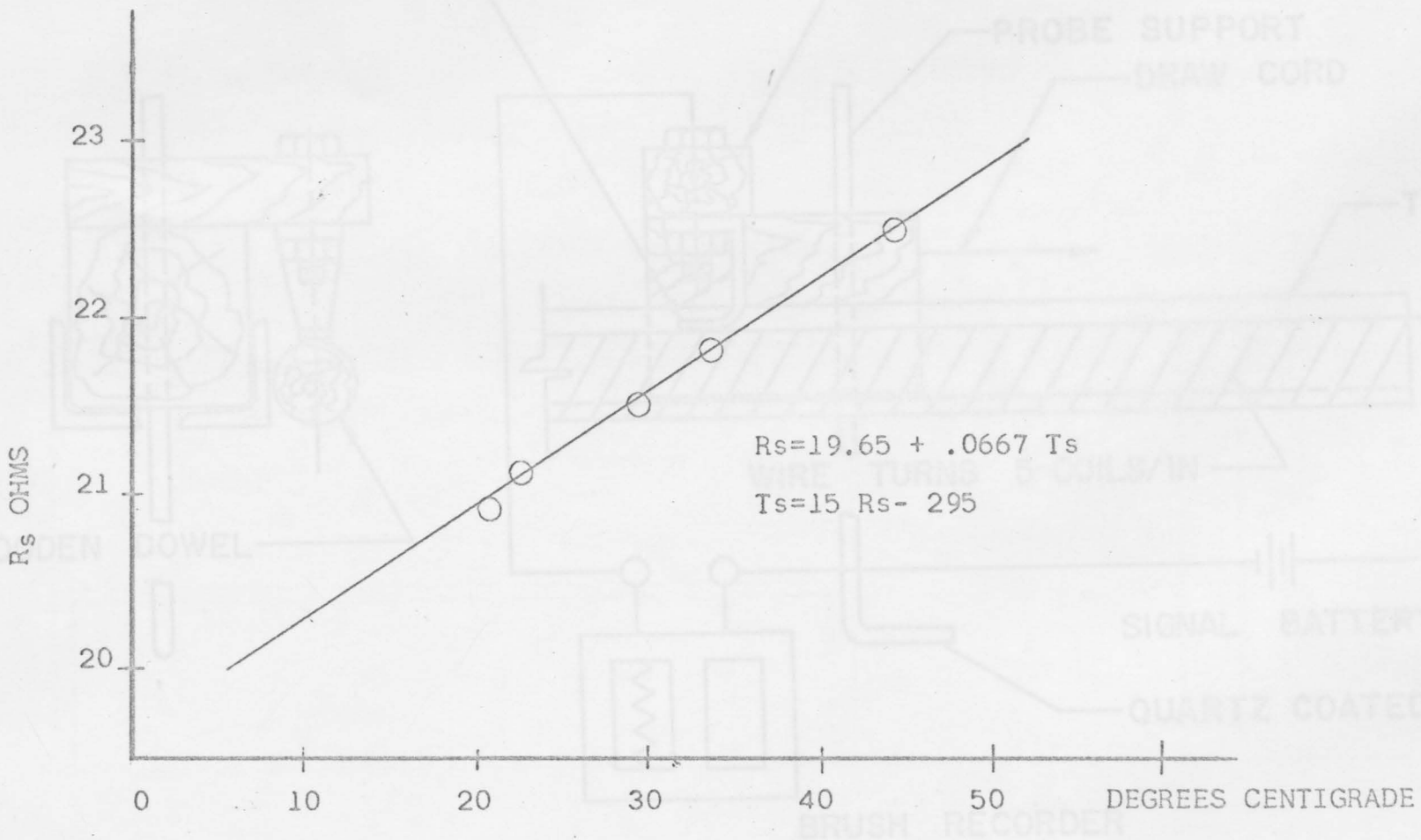

Fig.2. Probe Resistance vs Temperature

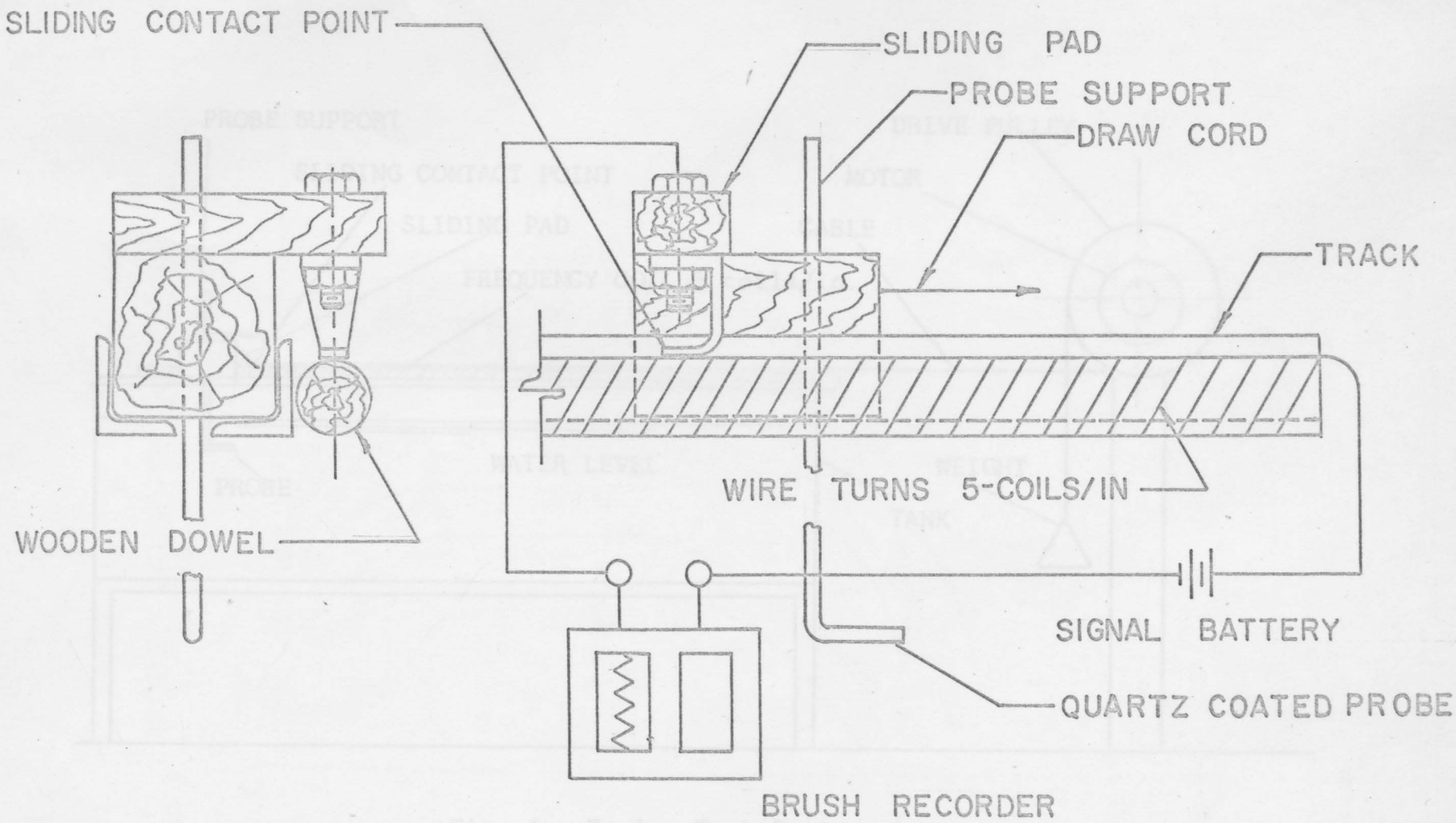

FIG. 3 CONTACT POINT AND COIL DRAWING.

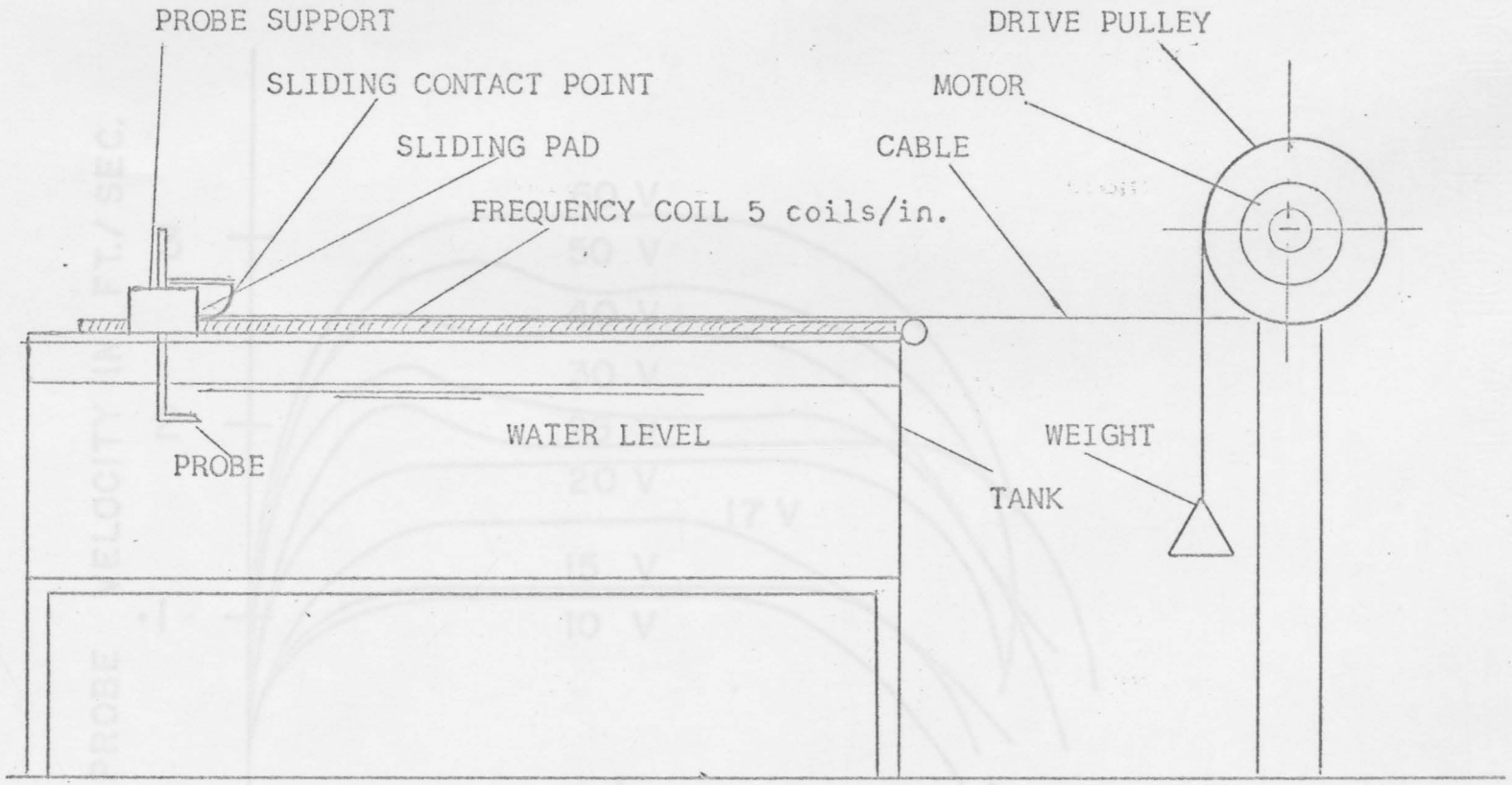

Fig. 4. Towing Tank System

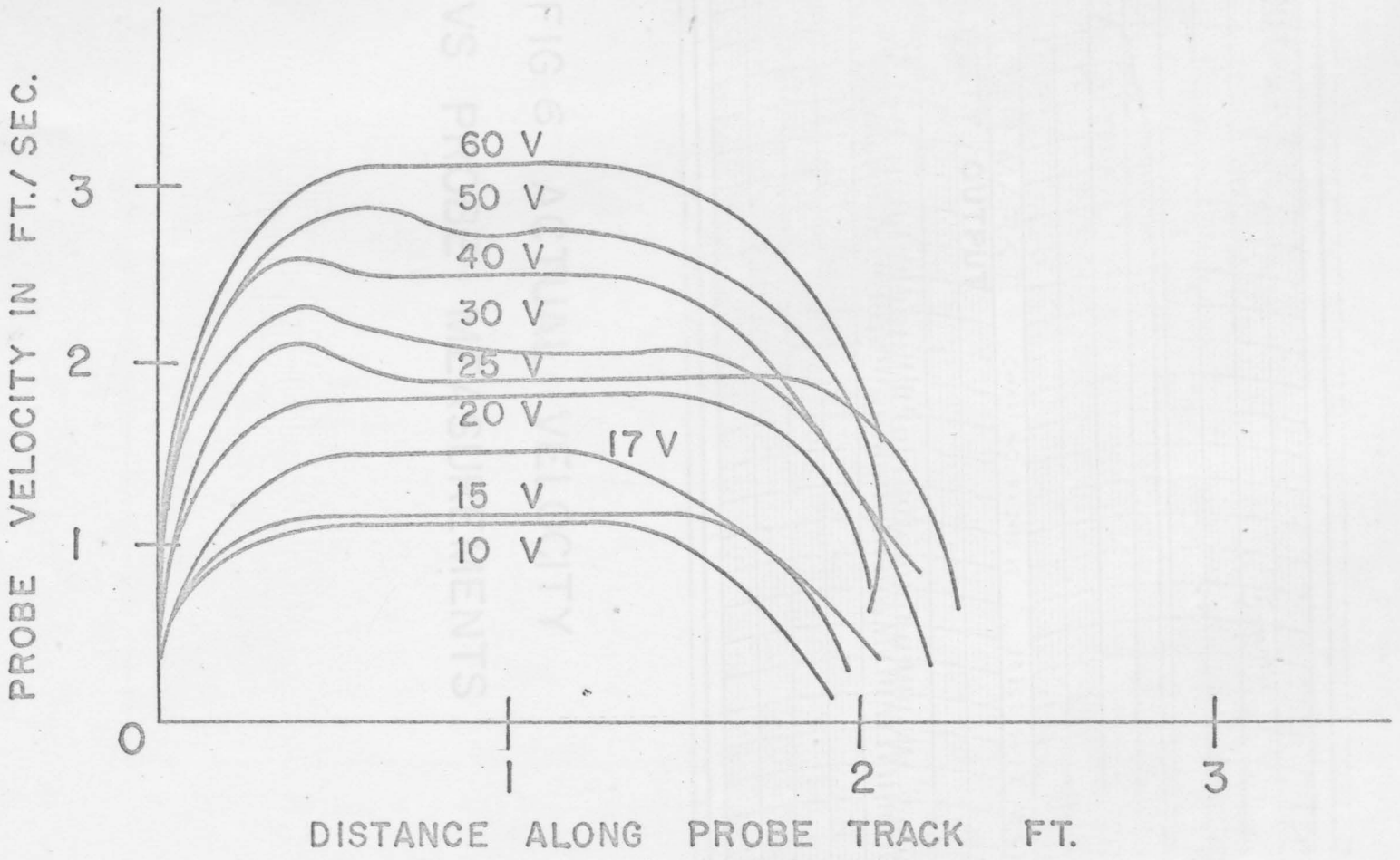

FIG.5 PROBE VELOCITY VS DISPLACEMENT

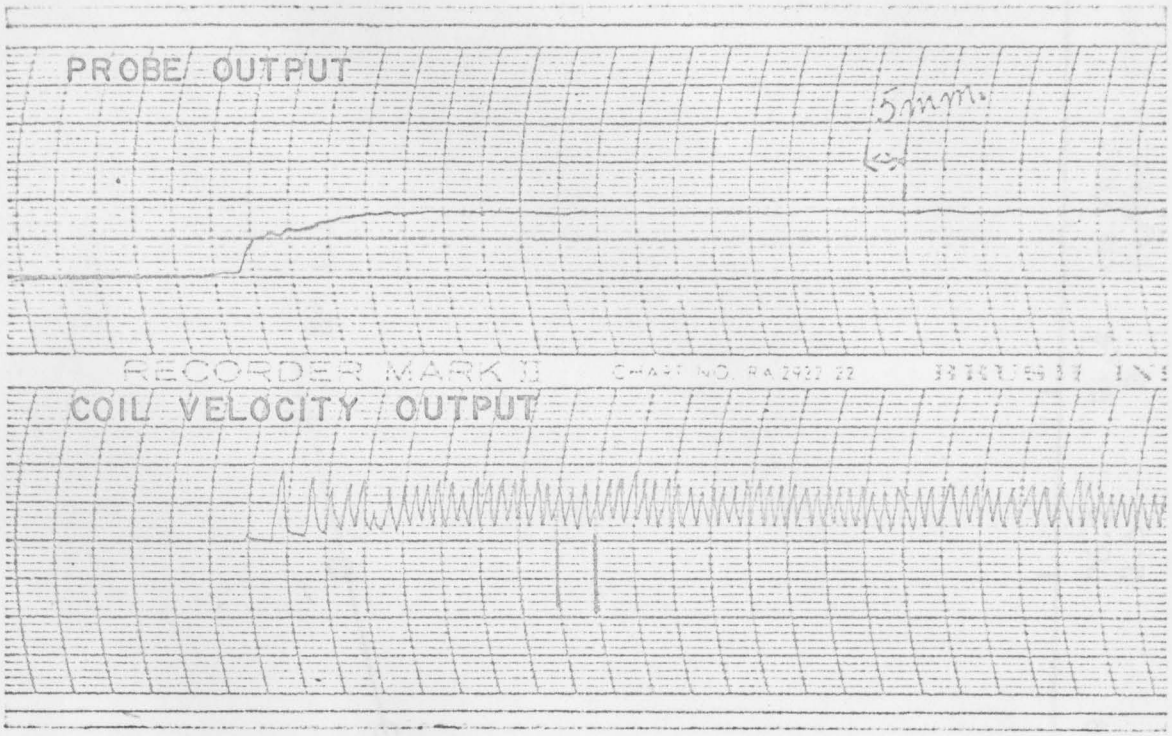

FIG 6 ACTUAL VELOCITY
VS PROBE MEASUREMENTS

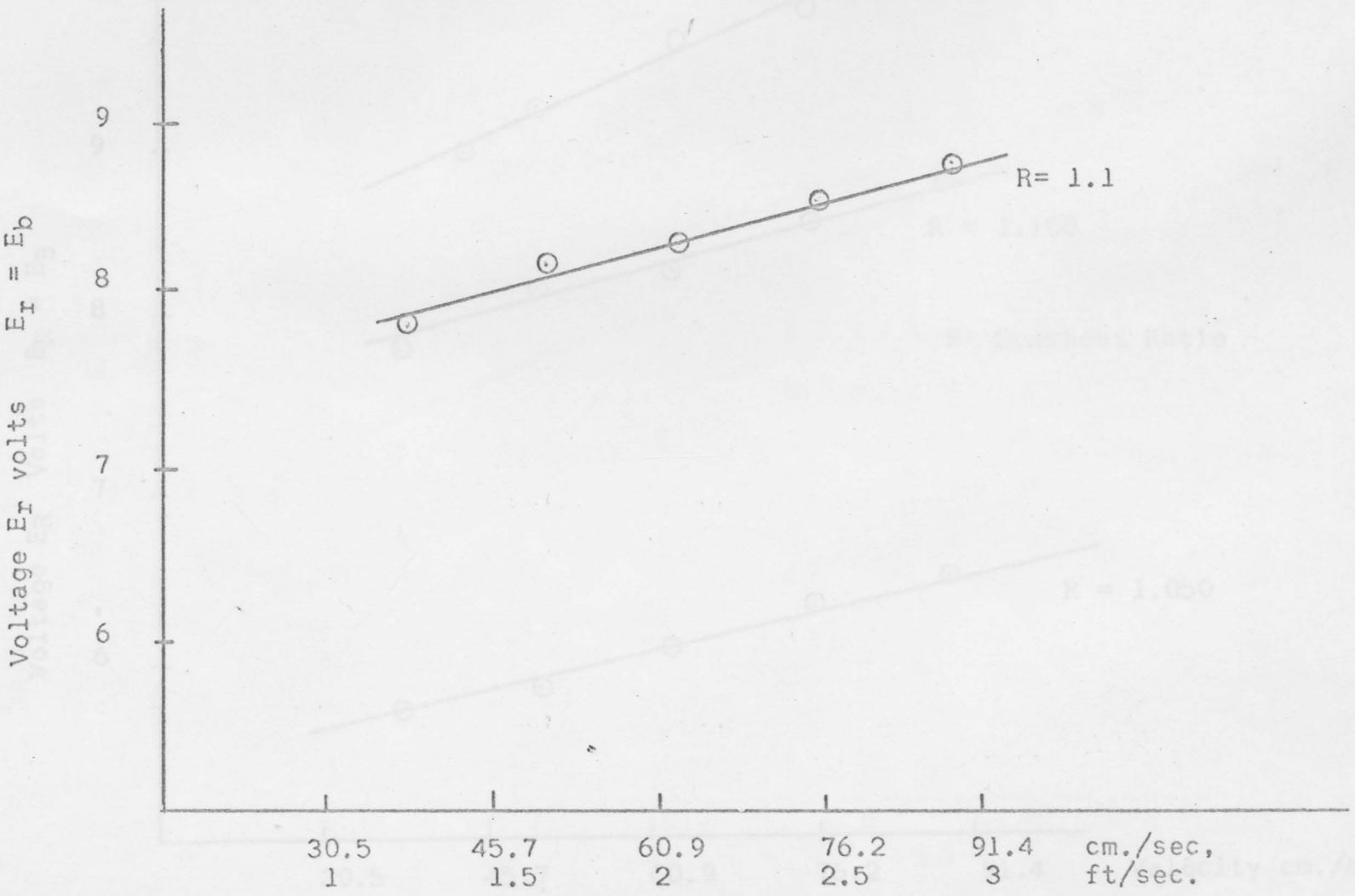

Fig. 7. Output Voltage vs Velocity

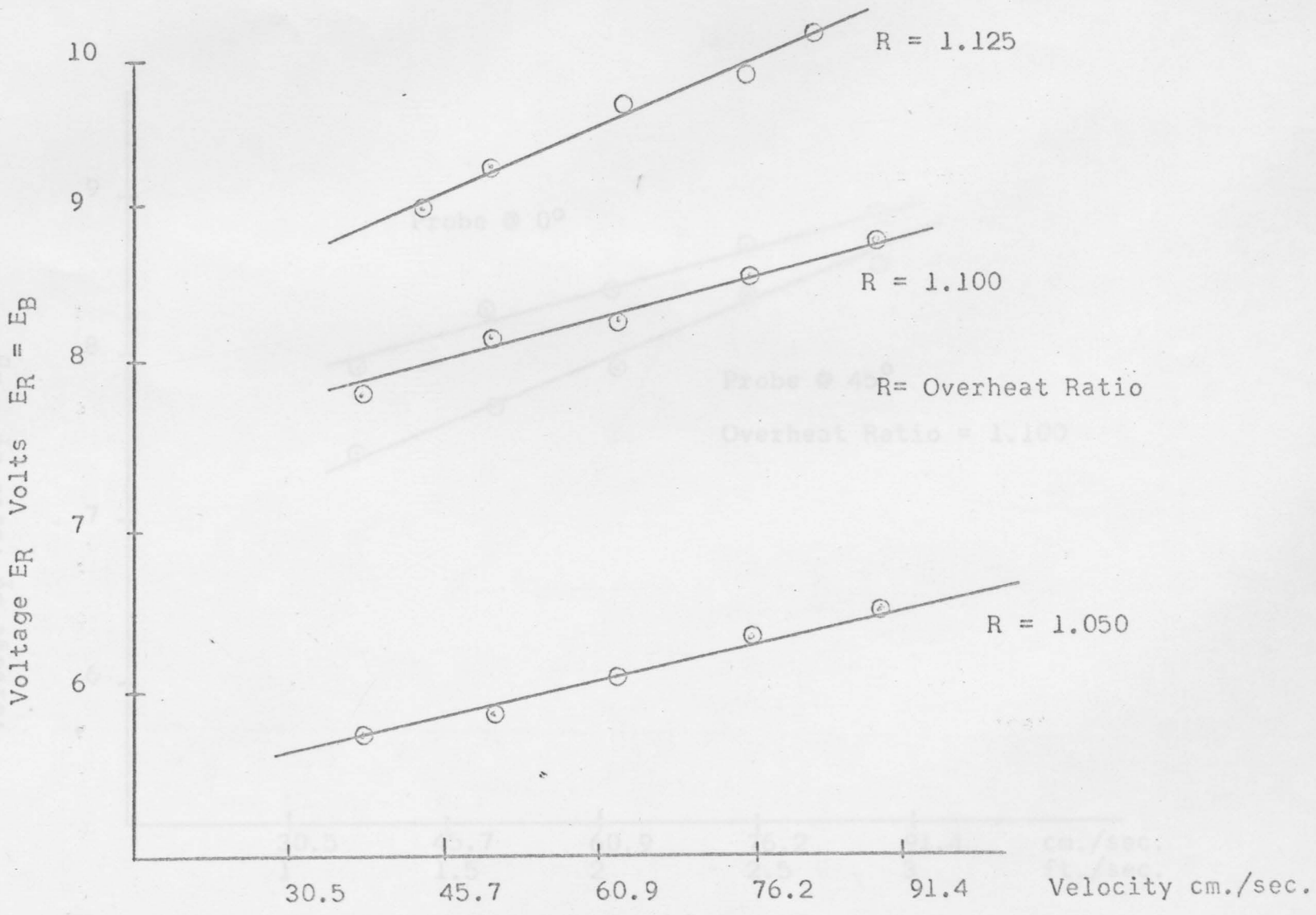

— Fig. 8. Output Voltage vs Velocity

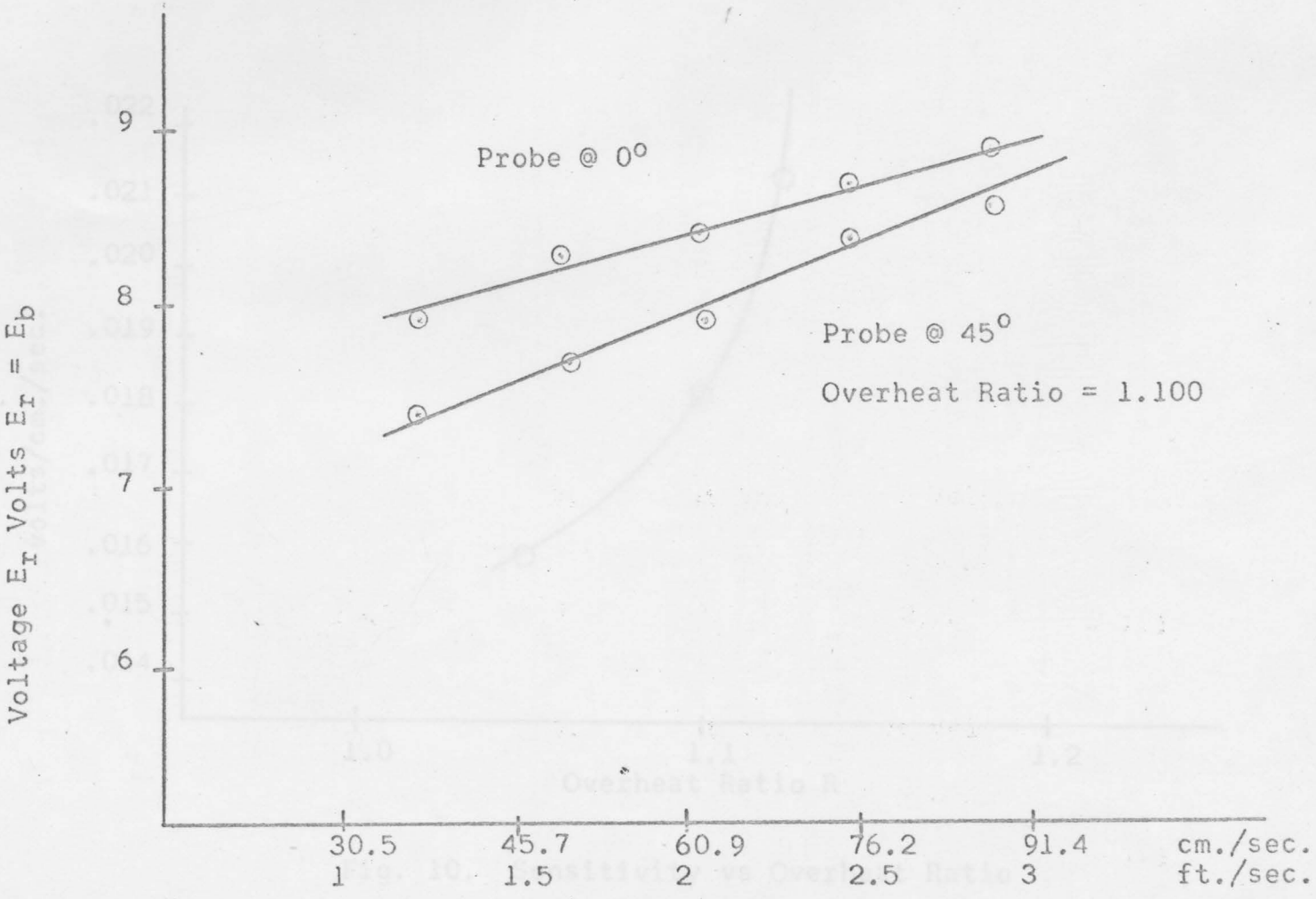

Fig. 9. Output Voltage vs Velocity

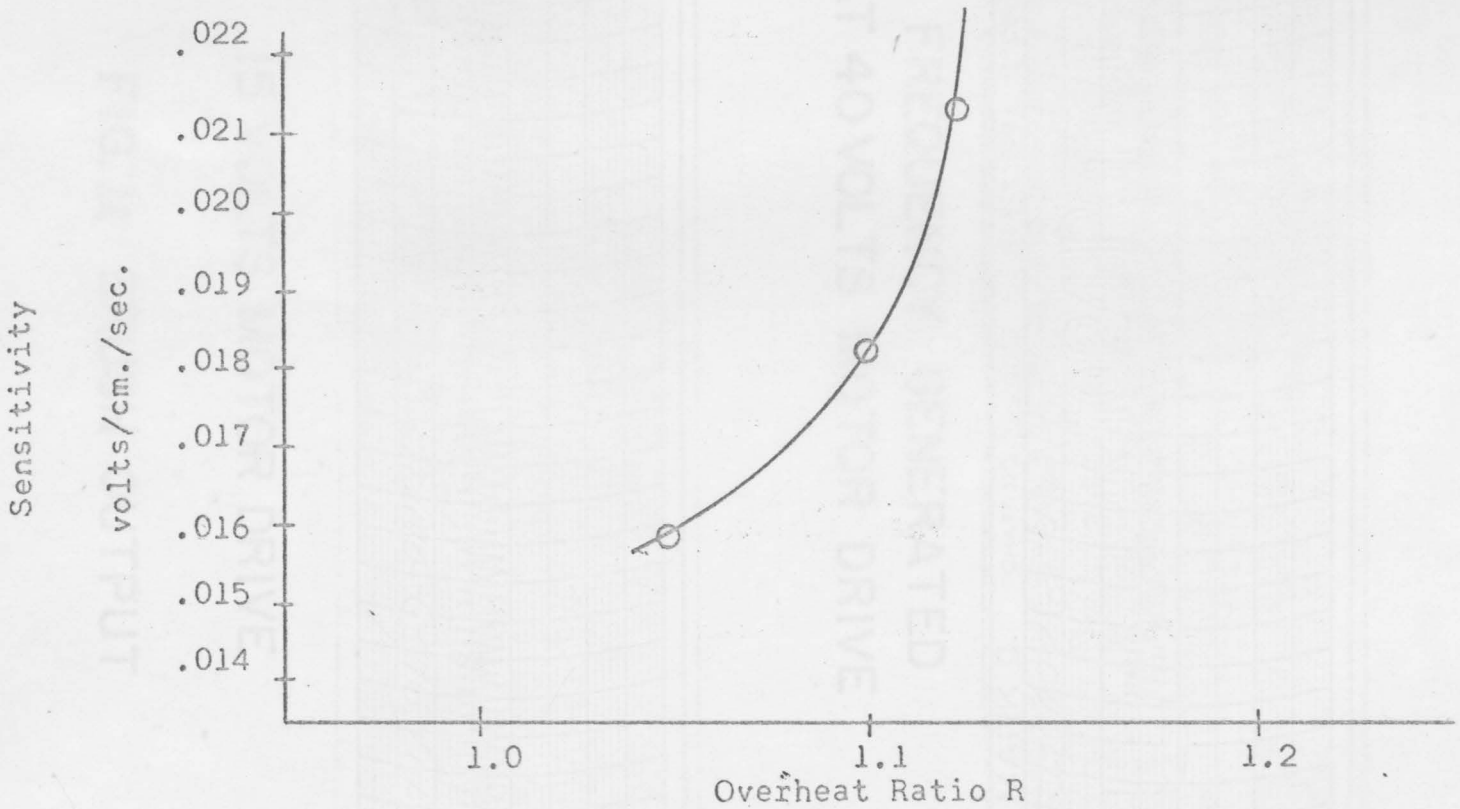

Fig. 10. Sensitivity vs Overheat Ratio

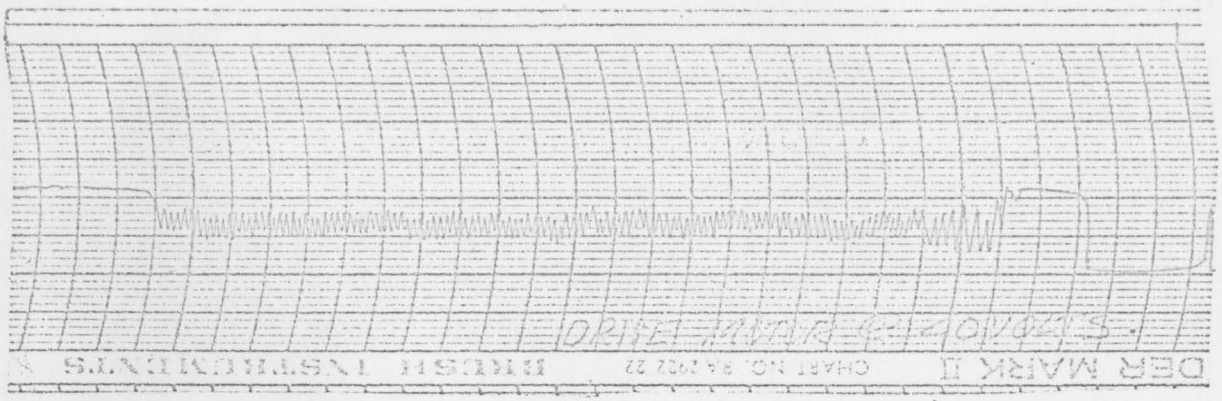

FREQUENCY GENERATED
AT 40 VOLTS MOTOR DRIVE

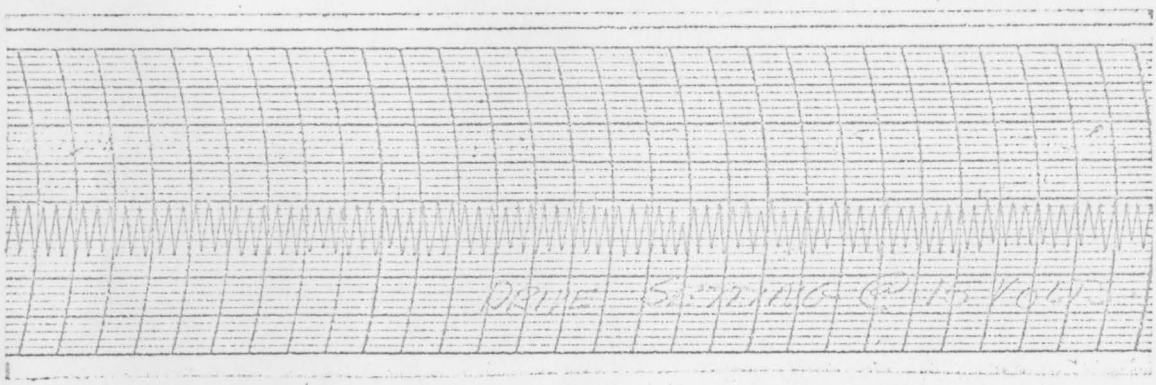

15 VOLTS MOTOR DRIVE

FIG. 11 BRUSH OUTPUT

APPENDIX B

Equipment List

EQUIPMENT LIST

Electric Motor	-	Bodine Model 321 WG093 1/8 Horse w/Gear Reduction
DISA Anemometer	-	Type 55D01
DISA Digital Voltmeter	-	Type 55D31
Brush Mark II Recorder		
Hewlett-Packard Oscilloscope	-	Type 175A-0
Signal Conditioner Aux. Unit	-	Unit 55D25